BBA - Molecular Basis of Disease 1865 (2019) 1402–1409

Contents lists available at ScienceDirect

BBA - Molecular Basis of Disease

journal homepage: www.elsevier.com/locate/bbadis

Inhibition of PRMT3 activity reduces hepatic steatosis without altering atherosclerosis susceptibility in apoE knockout mice

Menno Hoekstra*, Joya E. Nahon, Laura M. de Jong, Mara J. Kröner, Lidewij R. de Leeuw, Miranda Van Eck

Division of BioTherapeutics, Leiden Academic Centre for Drug Research, Gorlaeus Laboratories, Einsteinweg 55, 2333CC Leiden, the Netherlands.

ARTICLE INFO

Keywords:
Protein arginine methyltransferase
Atherosclerosis
Fatty liver disease
Hepatic steatosis
Pharmacological inhibition
Mouse model

ABSTRACT

The nuclear receptor liver X receptor (LXR) impacts on cholesterol metabolism as well as hepatic lipogenesis via transcriptional regulation. It is proposed that inhibition of the protein arginine methyltransferase 3 (PRMT3) uncouples these two transcriptional pathways in vivo by acting as a specific lipogenic coactivator of LXR. Here we validated the hypothesis that treatment with the allosteric PRMT3 inhibitor SGC707 will diminish the hepatic steatosis extent, while leaving global cholesterol metabolism, important in cholesterol-driven pathologies like atherosclerosis, untouched. For this purpose, 12-week old hyperlipidemic apolipoprotein E knockout mice were fed a Western-type diet for six weeks to induce both hepatic steatosis and atherosclerosis. The mice received 3 intraperitoneal injections with SGC707 or solvent control per week. Mice chronically treated with SGC707 developed less severe hepatic steatosis as exemplified by the 51% reduced ($P < 0.05$) liver triglyceride levels. In contrast, the extent of in vivo macrophage foam cell formation and aortic root atherosclerosis was not affected by SGC707 treatment. Interestingly, SGC707-treated mice gained 94% less body weight ($P < 0.05$), which was paralleled by changes in white adipose tissue morphology, i.e. reduction in adipocyte size and browning.

In conclusion, we have shown that through PRMT3 inhibitor treatment specific functions of LXR involved in respectively the development of fatty liver disease and atherosclerosis can be uncoupled, resulting in an overall diminished hepatic steatosis extent without a negative impact on atherosclerosis susceptibility. As such, our studies highlight that PRMT3 inhibition may constitute a novel therapeutic approach to limit the development of fatty liver disease in humans.

1. Introduction

Hepatic steatosis is a condition where neutral lipids in the liver accumulate [1]. Hepatic steatosis and related disorders are the most common form of liver disease [2]. The prevalence is rapidly growing as a result of the rising numbers of people with obesity and diabetes [3]. Augmented de novo hepatic lipogenesis, a process regulated by the nuclear receptor liver X receptor (LXR) is associated with an increased risk for hepatic steatosis [4]. The nuclear receptor stimulates the transcription of genes essential for de novo hepatic triglyceride synthesis: acetyl-CoA carboxylase (ACC1), fatty acid synthase (FAS), and stearoyl-coenzyme A desaturase 1 (SCD1) [5]. In addition, LXR is essential in hepatic and macrophage cholesterol metabolism [6]. Upon activation by its oxysterol ligands, LXR transcriptionally activates hepatic genes involved in the conversion of cholesterol to bile acid and the direct secretion of cholesterol into the bile, i.e. cholesterol 7α-hydroxylase, ATP-binding cassette (ABC) transporters G5 (ABCG5) and G8 (ABCG8). In macrophages, LXR stimulates the efflux of cellular cholesterol via ABCA1 and ABCG1 [7]. Thus, in contrast to LXR's harmful role in hepatic steatosis, LXR protects against atherosclerosis by decreasing the accumulation of cholesterol in macrophages and preventing foam cell formation [8]. Protein arginine *N*-methyltransferase 3 (PRMT3) acts as a specific cofactor for LXR transcription [9]. Studies by Kim et al. have shown that inhibition of PRMT3 function protects against hepatocyte triglyceride accumulation in vitro [9]. We have confirmed a potential role for PRMT3 in the development of hepatic

Abbreviations: ABC transporter, ATP-binding cassette transporter; ACC1, acetyl-CoA carboxylase 1; ADMA, asymmetric dimethylarginine; ALT, alanine aminotransferase; ApoE, apolipoprotein E; cCIMT, common Carotid Intima-Media Thickness; FAS, fatty acid synthase; LPL, lipoprotein lipase; LXR, liver X receptor; MCP1, monocyte chemoattractant protein 1; oxLDL, oxidized LDL; PRMT3, protein arginine methyltransferase 3; SDMA, symmetric dimethylarginine; SREBP-1c, sterol regulatory element-binding protein-1c; SCD1, stearoyl-coenzyme A desaturase 1; TNFα, tumor necrosis factor alpha; UCP1, uncoupling protein 1

* Corresponding author.
E-mail address: hoekstra@lacdr.leidenuniv.nl (M. Hoekstra).

https://doi.org/10.1016/j.bbadis.2019.02.012
Received 9 August 2018; Received in revised form 7 February 2019; Accepted 12 February 2019
Available online 15 February 2019
0925-4439/

steatosis in a short-term in vivo setting [10]. More specifically, mice treated with the selective PRMT3 antagonist SGC707 were protected from fatty liver development induced by LXR activation using T0901317 and palm oil [11]. Importantly, we noticed that the anticipated reduction in LXR activity upon SGC707 treatment was selective for the hepatic lipogenesis genes, as the LXR-driven genes involved in cholesterol metabolism were not affected by pharmacological blockade of PRMT3 activity. Uncoupling of the two LXR activities is interesting in light of potential therapeutic use of the SGC707 compound. Treatment with SGC707 could theoretically diminish hepatic steatosis, while leaving hepatic and macrophage cholesterol metabolism, important in cholesterol-driven pathologies like atherosclerosis, untouched. To validate this hypothesis, the effect of chronic PRMT3 inhibition through SGC707 treatment was investigated in atherosclerosis-susceptible hyperlipidemic apolipoprotein E (apoE) knockout mice.

2. Materials and methods

2.1. Mice

Animal experiments were approved by the Ethics Committee for Animal Experiments of Leiden University and performed at the Gorlaeus Laboratories of the Leiden Academic Centre for Drug Research in accordance with the National Laws and the Directive 2010/63/EU of the European Parliament. Animal studies are reported in compliance with the ARRIVE guidelines.

ApoE knockout mice were originally obtained from The Jackson Laboratory (The Jackson Laboratory, Bar Harbor, ME, USA) and subsequently bred in house to expand the colony. Twelve week-old male apoE knockout mice weighing on average 30.8 ± 0.5 g were challenged with a Western-type diet (0.25% cholesterol and 15% cocoa butter, SDS, Sussex, UK) for 6 weeks to induce atherosclerotic lesion development. During this period, the mice received 3 intraperitoneal injections with SGC707 (10 mg kg^{-1}; N = 12) or a similar amount of solvent control (10 µl DMSO; N = 12) per week. Mice were randomly distributed over the two treatment groups. Body weight was monitored twice weekly. Over the course of the study, 3 control mice developed severe skin wounds, which led to elimination of these mice from the study. After the 6-week intervention period, the remaining 21 mice (SGC707 group: N = 12; controls group: N = 9) were bled in EDTA-coated vials via tail incision for plasma lipid and hematological analysis and anaesthetized by subcutaneous injection with a mix of 70 mg kg^{-1} body weight xylazine, 1.8 mg kg^{-1} bodyweight atropine and 350 mg kg^{-1} body weight ketamine. Animals were subsequently killed by cervical dislocation. The arterial tree was perfused in situ with PBS (100 mmHg) for 10 min via a cannula in the left ventricular apex. The heart plus aortic root, liver, kidneys and gonadal white adipose tissue were excised and stored in 3.7% neutral-buffered formalin (Formal-fixx; Shandon Scientific Ltd., Runcorn, UK) for 24 h or stored at −20° until further use.

2.2. Tissue lipid extraction and quantification

Triglycerides were extracted from liver and white adipose tissue using Nonidet™ P 40 Substitute (Sigma-Aldrich Corp.). In brief, approximately 50 mg of tissue was homogenized with 500 µl of Nonidet™ P 40 Substitute, heated until 90 °C and chilled on ice. The heating and cooling procedure was repeated once more to solubilize all triglycerides All insoluble material was removed by centrifuging at 13148 × *g*. The concentration of triglycerides was determined by the use of an enzymatic colorimetric assay. Cholesterol was extracted from liver tissue using the Folch extraction method [12]. The concentration of free cholesterol and cholesteryl esters in livers was determined by the use of enzymatic colorimetric assays as described by Out et al. [13]. The concentration of triglycerides, free cholesterol and cholesteryl esters was corrected for the total protein concentration, determined using a Pierce™ BCA Protein Assay Kit (ThermoFisher Diagnostics, Waltham, MA, USA).

2.3. Plasma measurements

Concentrations of total cholesterol and triglycerides in plasma specimens were determined using enzymatic colorimetric assays (Roche Diagnostics). The distribution over the different lipoproteins was analyzed by fractionation of 30 µl of plasma of each mouse using a Superose 6 column (3.2 × 300 mm, Smart-system, Pharmacia). Plasma alanine aminotransferase (ALT) levels were measured using Reflotron test strips (Roche Diagnostics) according to the suppliers instructions at the Gaubius building of TNO (Leiden, The Netherlands).

2.4. Hematological analysis

Total leukocyte numbers in whole blood samples with EDTA anticoagulant obtained at sacrifice were routinely measured using an automated Sysmex XT-2000iV Veterinary Hematology analyzer (Sysmex Corporation). Verification of effects on specified white blood cell subclasses was performed using fluorescence activated cell sorting (FACS analysis) by staining cells with appropriate antibodies (CD11b, Ly6G, CD4, CD8, CD19, CD86, CD62L, all obtained from eBioscience, Belgium). For this purpose, blood was lysed using 0.83% NH_4CL in 0.01 M Tris/HCL pH 7.2. Subsequently, 300.000 cells were stained with the indicated antibodies. FACS analysis was performed on the FACSCalibur II (Becton Dickinson, Mountain View, CA). Identification of specific leukocyte subsets was primarily based upon the indicated fluorescent antibody signals, but was further validated by checking the size and granularity of the tagged cells in the forward/side scatter plots. Data were analyzed using FlowJo software. Peritoneal leukocytes were obtained by lavaging the peritoneal cavity of the mice with 10 ml of ice-cold PBS. The percentage of foam cells in the total leukocyte population was analyzed as described previously [14]. More specifically, peritoneal cells displaying a high fluorescent signal in both forward-scattered light (FSC) and side-scattered light (SSC) channels of the Sysmex apparatus were labeled macrophage foam cells.

2.5. Histological analysis

Serial sections (10 µm) of the aortic root were cut using a Leica CM3050S cryostat. The atherosclerotic lesion areas in Oil red O-stained cryostat sections of the aortic root were quantified, in a blinded manner, using the Leica image analysis system, consisting of a Leica DMRE microscope coupled to a video camera and Leica Qwin Imaging software (Leica Ltd., Cambridge, UK). Mean lesion area (in μm^2) was calculated from 5 consecutive sections of the aortic root, starting at the appearance of the tricuspid valves. Cryosections of the liver (7 µm) were generated and evaluated for the presence of neutral lipid using Oil red O staining (Sigma-Aldrich, Zwijndrecht, The Netherlands). Paraffin embedded liver and white adipose tissue was cut serially using a RM2235 rotary microtome (Leica Ltd., Cambridge, UK) at intervals of 6 µm. The sections were subsequently routinely stained with hematoxilin (Sigma-Aldrich, Zwijndrecht, The Netherlands) and eosin (Merck, Darmstadt, Germany). Liver paraffin sections were subjected to Masson's Trichrome staining (Sigma-Aldrich, Zwijndrecht, The Netherlands) to visualize collagen deposits (blue colour). Representative images were obtained using the Leica image analysis system. The number of adipocytes in white adipose tissue was manually quantified within fixed areas (N = 3 per group).

2.6. Analysis of gene expression by real-time quantitative PCR

Quantitative gene expression analysis was performed as described [15]. Total RNA was isolated according to Chomczynski and Sacchi [16] and reverse transcribed using RevertAid™ reverse transcriptase.

Gene expression analysis was performed using real-time SYBR Green technology (Eurogentec). Primer sequences are available on request. Beta-actin, ribosomal protein L27, peptidylprolyl isomerase A, glyceraldehyde 3-phosphate dehydrogenase, and acidic ribosomal phosphoprotein P0 were used as the standard reference genes. Genes were considered as being not expressed when they exhibited a Ct value of > 35.

2.7. Microarray-based analysis of macrophage PRMT3 expression under basal and atherogenic conditions

To generate bone marrow-derived macrophages, bone marrow cells were isolated from femurs of C57BL/6 mice and cultured for 7 days in complete RPMI medium supplemented with 20% FCS and 30% L929 cell-conditioned medium as a source of macrophage colony-stimulating factor. After harvesting, cells were cultured overnight in DMEM containing 10% FCS. Subsequently, cells were exposed to DMEM containing 0.2% BSA with or without addition of foam cell inducing oxidized LDL (oxLDL; 20 ng/ml) for 48 h. A RNAeasy mini kit (Qiagen, Chatsworth, CA) was used to isolate total RNA (N = 3 per group). After checking the concentration and integrity of the RNA and an amplification step (Ambion, #IL1791), the MouseWG-6 v2.0 microarray was performed according to manufacturer's specifications (Illumina, San Diego, CA). Probe ID 1990152 represented PRMT3. A relative expression level of > 80 arbitrary units was necessary for a transcript to be considered as reliably detected.

2.8. Statistical analysis

Data are presented as means ± SEM or means plus individual data points. Statistical analysis was performed using Graphpad Instat software (San Diego, USA, http://www.graphpad.com). Normality testing of the experimental groups was performed using the method Kolmogorov and Smirnov (Graphpad Instat). The significance of differences was calculated using a two-tailed Student's *t*-test or two way analysis of variance (ANOVA) with Bonferroni post-test where appropriate. Probability values < 0.05 were considered significant.

3. Results

3.1. Chronic PRMT3 inhibition reduces hepatic steatosis in apoE knockout mice

Western-type diet-fed apoE × LXRalpha double knockout mice display whole body cholesterol accumulation and an increased atherosclerosis susceptibility as compared to apoE single knockout mice [17], suggesting an important physiological role for endogenous LXR activation in apoE knockout mice during Western-type diet feeding. SGC707 is an allosteric inhibitor of PRMT3 that does not impact the activity for 31 other methyltransferases and > 250 non-epigenetic targets [18]. To establish that PRMT3 inhibition can diminish the Western-type diet-induced (LXR-driven) hepatic steatosis development, we investigated liver morphology in atherogenic diet-fed apoE knockout mice after 6 weeks of parallel treatment with SGC707. Absolute liver weight of SGC707-treated animals was significantly lower than in solvent control-treated mice (−13%; P < 0.05; Fig. 1A). However, after correcting the liver weight for total body weight the significance between the two groups was lost (5.4 ± 0.2% for SGC707-treated mice versus 5.6 ± 0.3% for controls, respectively; P > 0.05). As can be appreciated from the representative pictures in Fig. 1B, control-treated mice apoE knockout mice developed fatty livers. More specifically, significant macrovesicular steatosis was visible in hematoxylin/eosin-stained liver paraffin sections from control-treated mice (Fig. 1B; middle panels). Oil red O staining of cryosections validated the presence of large neutral lipid deposits (Fig. 1B; right panels). In accordance with the notion that mice only suffered from early stage fatty liver disease (simple steatosis), we did not observe the hepatocellular ballooning or intralobular inflammation phenotypes typically seen with non-alcoholic steatohepatitis [3,19]. All liver sections stained with Masson's Trichrome were negative for collagen (Fig. 1B; left panels), which highlights the absence of non-alcoholic steatohepatitis-associated fibrosis. Importantly, as also evident from Fig. 1B, mice chronically treated with SGC707 had developed less severe hepatic steatosis. In contrast to the macrovesicular disease phenotype of control-treated mice, SGC707-treated animals rather suffered from microvesicular steatosis. As a result, only a limited amount of neutral lipid stores could be found in Oil red O-stained liver sections of SGC707-treated mice. Plasma levels of the hepatotoxicity marker alanine aminotransferase (ALT) tended to be lower after SGC707 treatment (−27%; P = 0.09; Fig. 1C). Previous studies by Craig et al. have shown that changes in absolute kidney weight reliably predict the occurrence of kidney toxicity [20]. Absolute kidney weights were not significantly different in SGC707-treated mice (248 ± 9 mg) as compared to control-treated mice (270 ± 16 mg). It can therefore be suggested that the observed decrease in hepatic steatosis extent was not secondary to a (systemic) toxic effect of SGC707 treatment. Chronic SGC707 exposure was also not associated with the induction of liver inflammation. As such, hepatic gene expression levels of the inflammatory cytokines monocyte chemoattractant protein 1 (MCP1) and tumor necrosis factor alpha (TNFα) and the macrophage marker CD68 were not different between SGC707-treated and control mice (Fig. 1D). Quantification of the different major lipid species showed that livers of SGC707-treated mice contained markedly less triglycerides (−51%; P < 0.05) as compared to control mice (Fig. 1E). Hepatic free cholesterol (Fig. 1E) and cholesteryl esters (Fig. 1E) levels were not different between both groups, suggesting that the reduction in hepatic neutral lipid accumulation was driven by a decrease in liver triglycerides.

3.2. Chronic PRMT3 inhibition does not impact the lipoprotein profile in apoE knockout mice

In line with our previously published data in the short-term model for murine hepatic steatosis [10], the changes in liver lipid status were not paralleled by a change in plasma lipid levels. SGC707-treated mice had similar plasma triglyceride (Fig. 2A) and total cholesterol (Fig. 2B) levels. The distribution of the plasma cholesterol over the lipoprotein fractions was also not markedly different in the two groups of mice (Fig. 2C).

3.3. Chronic PRMT3 inhibition does not change the immune status of apoE knockout mice

Protein arginine methyltransferase 1 (PRMT1), a family member of PRMT3, modulates immune cell activation [21,22]. Although an immune function has not yet been described for PRMT3, we determined circulating leukocyte numbers and measured their activation status to exclude that a cholesterol-independent immune modulatory effect of PRMT3 is relevant in context of the development of atherosclerotic lesions. Total circulating leukocytes were similar in both the SGC707-treated group and the control group (Fig. 3A). Within the blood leukocyte populations, a minor increase in the relative fraction of CD4+ T-cells was detected in the mice treated with the PRMT3 inhibitor as compared to controls (P < 0.05; Fig. 3B). It is generally assumed that the activation and differentiation state of T-cells in atherosclerosis is more important than their quantity [23,24]. Importantly, the distribution of CD4+ T-cells over the naïve, effector and memory effector subsets was similar between both groups of mice (Fig. 3C).

3.4. Chronic PRMT3 inhibition does not change the foam cell extent or atherosclerosis susceptibility in apoE knockout mice

Given that the SGC707 treatment did not impact on hepatic

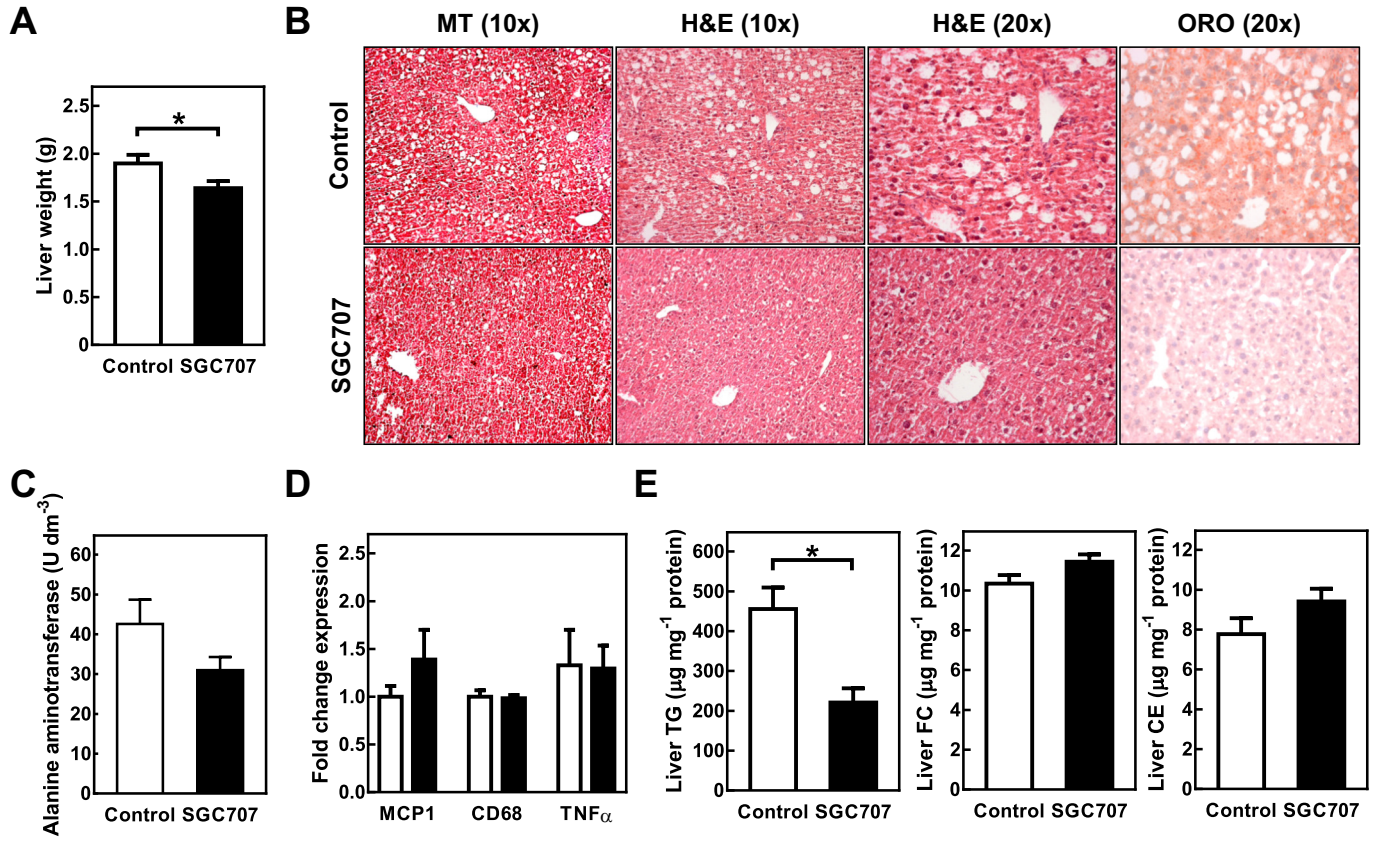

Fig. 1. Reduced accumulation of triglycerides in the liver in SGC707-treated apoE knockout mice. A) SGC707-treated mice showed a lower liver weight as compared to control mice. B) Representative micrographs of livers stained with Masson's Trichrome (MT) for collagen, hematoxylin and eosin (H&E) and Oil red O (ORO) for neutral lipids. C) Plasma alanine aminotransferase levels were not different. C) The change in steatosis extent was not accompanied by a change in the relative mRNA expression levels of the inflammation markers monocyte chemoattractant protein 1 (MCP1), macrophage marker CD68 and tumor necrosis factor alpha (TNFα). D) Liver triglycerides, but not free cholesterol and cholesteryl esters, were lower in SGC707-treated mice as compared to control mice. Black bars: SGC707 treated mice; N = 12. White bars: control treated mice; N = 9. Graphs represent means ± SEM. * P < 0.05. (For interpretation of the references to colour in this figure legend, the reader is referred to the web version of this article.)

cholesterol levels, we verified that macrophage cholesterol metabolism was also not changed in response to chronic PRMT3 inhibition. Notably, as can be appreciated from our microarray findings displayed in Supplemental Fig. 1, PRMT3 expression can be reliably detected in bone marrow-derived macrophages already under control culture conditions and PRMT3 levels actually increase under pro-atherogenic conditions, i.e. during oxLDL-induced foam cell formation. However, the percentage of macrophage foam cells in the peritoneal cavity was similar after treatment of Western-type diet-fed apoE knockout mice with SGC707 (Fig. 4A). This latter finding provides support for our notion that the beneficial effect of LXR in the protection against foam cell formation was not disrupted by the SGC707-mediated inhibition of PRMT3 activity. To validate that the similar extent of foam cell formation also translated into an unchanged atherosclerosis susceptibility, we measured the atherosclerosis extent in the aortic root. Solvent control-treated apoE knockout mice had developed initial atherosclerotic lesions with an average lesion area of 173 ± 22 ∗ 10^3 µm^2 after 6 weeks on the Western-type diet. In concordance with the unchanged plasma cholesterol, circulating leukocytes and foam cell numbers, atherosclerotic lesions in the aortic root of SGC707-treated mice stained with Oil red O for neutral lipids looked similar, as can be appreciated from Fig. 4B. Quantification showed that the Oil red O-

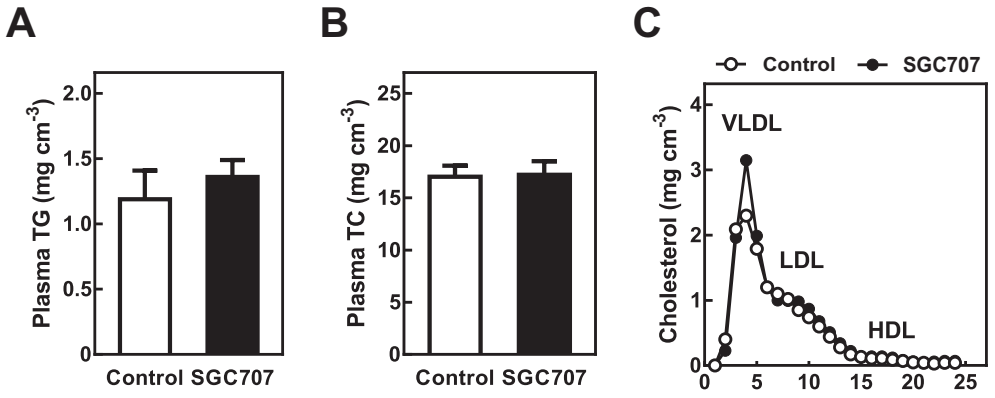

Fig. 2. SGC707 treatment did not affect plasma lipids in apoE knockout mice. A) Plasma triglyceride (TG) and B) total cholesterol (TC) levels were not different in SGC707-treated mice and the control group. C) The distribution of cholesterol over the different lipoprotein fractions in plasma, including very-low-density lipoprotein (VLDL), low-density lipoprotein (LDL) and high-density lipoprotein (HDL) was similar in both groups (N = 3 per group). Black bars: SGC707-treated mice; N = 12. White bars: control treated mice; N = 9. Graphs represent means ± SEM.

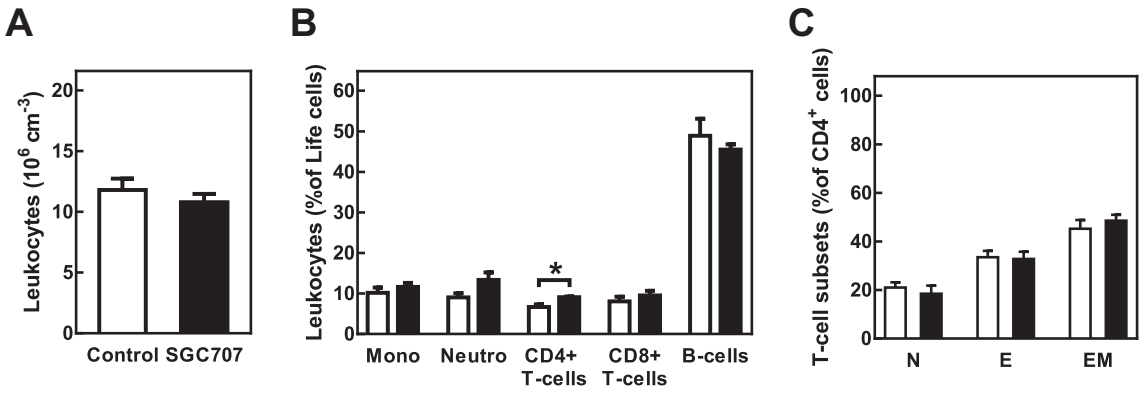

Fig. 3. No functional changes in circulating leukocytes in SGC707-treated apoE knockout mice. A) Total circulating leukocyte numbers were not different between the two experimental groups. B) The distribution of the leukocytes over the different cell subsets showed only a minor increase in CD4+ T-cells in SGC707-treated mice as compared to control treated mice. C) The activity of the CD4+ T-cells was not affected by SGC707 treatment. Black bars: SGC707 treated mice; N = 12. White bars: control treated mice; N = 9. Graphs represent means ± SEM. * $P < 0.05$.

positive lesion area was indeed not different in SGC707-treated mice as compared to controls (146 ± 17 ∗ 10^3 μm^2; Fig. 4C). Relative expression levels of the macrophage marker CD68 were determined in the aortic arch as measure for initial atherosclerotic lesion development in a second location. The results from the aortic root showing a null effect of SGC707 treatment on atherosclerosis outcome were supported by the similar gene expression levels of CD68 in the aortic arch of the two groups of mice (Fig. 4D). Aortic PRMT3 gene expression levels were measured to exclude that the null effect on atherosclerosis after SGC707 treatment was due to the fact that PRMT3 was not present locally in the diseased vessel wall. In control mice, relative mRNA expression levels of PRMT3 within the aortic arch were about half of those found in the liver (0.0015 ± 0.0005 for aorta and 0.0034 ± 0.0002 for liver, respectively). PRMT3 mRNA expression levels in aortic and liver specimens of SGC707-treated mice were essentially the same as those in control mice (0.0014 ± 0.0003 for aorta and 0.0037 ± 0.0002 for liver). This latter finding highlights that chronic SGC707 treatment was not associated with a compensatory feedback on the rate of PRMT3 gene transcription.

3.5. Chronic PRMT3 inhibition reduces weight gain in apoE knockout mice

Notably, we observed a 94% reduced ($P < 0.05$) body weight gain upon Western-type diet feeding in the mice treated with SGC707 as compared to control mice (Fig. 5A and B). Adipocytes in gonadal white adipose tissue of SGC707-treated mice appeared slightly smaller during tissue histological observation (Fig. 5C). In line with an anticipated lower adipocyte volume, the number of adipocytes per quantified gonadal white adipose area was higher in SGC707-treated mice (93 ± 4 for SGC707-treated mice versus 76 ± 7 for controls; $P < 0.05$). Browning was not visible in any of the gonadal white adipose tissue sections. In accordance, gene expression of the classical brown adipose tissue marker uncoupling protein 1 (UCP1) could not be measured in ~50% of the white adipose tissue samples (independent of the treatment) and was equally low in the two groups of samples where UCP1 levels could be reliably detected (data not shown). In contrast, UCP1 mRNA expression levels were increased by 17-fold ($P < 0.05$) in subcutaneous white adipose tissue upon SGC707 treatment (Fig. 5D). Histological analysis of the subcutaneous white adipose tissue depots showed significant browning in the SCG707-treated mice. As evident from Fig. 5C, adipocytes in subcutaneous white adipose tissue of SCG707-treated mice generally appeared to be smaller. Furthermore, the appearance of adipocytes in several parts within the subcutaneous white fat depot was more reminiscent of brown adipocytes.

Previous studies in cultured adipocytes and wild-type and LXR knockout mice have suggested that LXR not only controls the transcription of the lipogenic transcription factor SREBP-1c in hepatocytes but also in adipocytes/adipose tissue [25,26]. As can be appreciated from the gonadal white adipose tissue gene expression profile in Fig. 5E, levels of SREBP-1c and the lipogenesis genes FAS, ACC1, and SCD1 were not significantly altered by SGC707 treatment. In contrast, SGC707 treatment was associated with a significant decrease (−48%; $P < 0.05$) in the mRNA expression levels of lipoprotein lipase (LPL) that, in adipocytes, facilitates the local catabolism of lipoprotein-

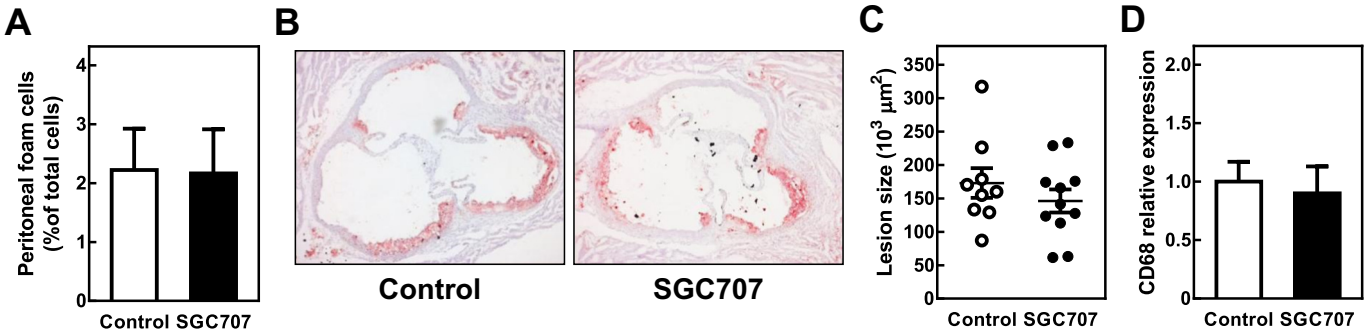

Fig. 4. SGC707 treatment did not affect foam cell formation or atherosclerosis susceptibility in apoE knockout mice. A) The quantity of foam cells as percentage of total peritoneal leukocytes was not different in the SGC707-treated mice and control mice. B) Representative micrographs of the aortic root stained with Oil red O for neutral lipids (red) 5× objective. C) The aortic atherosclerotic lesion area did not differ significantly between SGC707-treated mice (black circles) and the control group (white circles). D) Relative gene expression of CD68 in the aortic arch was similar in both groups. Black bars: SGC707-treated mice; N = 12. White bars: control treated mice; N = 9. Graphs represent means ± SEM. (For interpretation of the references to colour in this figure legend, the reader is referred to the web version of this article.)

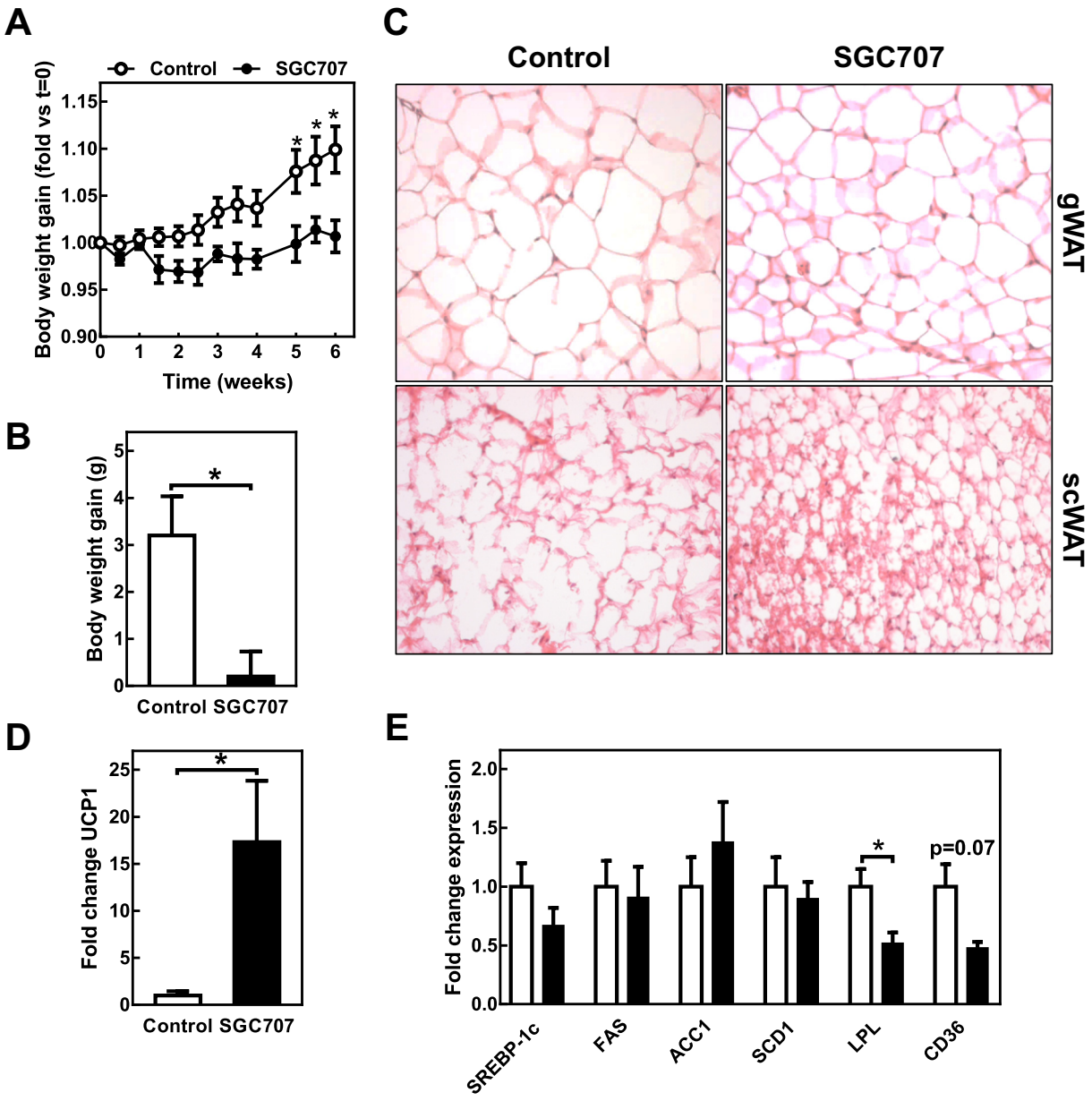

Fig. 5. SGC707 treatment attenuated body weight gain of apoE knockout mice. A) SGC707-treated mice (black circles) gained less weight during 6 weeks of Western-type diet feeding as compared to control mice (white circles). Data are expressed as fold change versus the starting weight. B) Absolute body weight gain was significantly reduced in SGC707-treated mice. C) Representative micrographs of white adipose tissue of both groups. D) White adipose tissue triglyceride (TG) levels, corrected for the amount of protein, tended to be lower in SGC707-treated mice as compared to control mice. E) SGC707-treated mice tended to have smaller adipocytes, as the number of cells per quantified area was slightly increased (N = 3 per group). F) Relative expression levels of lipolysis and fatty acid uptake but not lipogenesis genes were lower in SGC707-treated mice. Black bars: SGC707-treated mice; N = 12. White bars: control treated mice; N = 9. Graphs represent means ± SEM. * P < 0.05.

associated triglycerides for subsequent cellular uptake of the liberated fatty acids. Importantly, the decrease in LPL expression was paralleled by a clear trend towards a decrease (−52%; P = 0.07) in the relative expression level of the scavenger receptor CD36 that mediates the actual uptake of lipoprotein-derived fatty acids.

4. Discussion

Previously published in vitro and in vivo studies have proposed that PRMT3 is a coactivator for LXR that modulates LXR's lipogenic but not its function in cholesterol metabolism [9,10]. Here we show that chronic treatment of hyperlipidemic apoE knockout mice with the PRMT3 inhibitor SGC707 reduced the hepatic steatosis extent, while atherosclerotic lesion development was not negatively affected. This finding provides further evidence that through PRMT3 inhibition the LXR-driven (pathological) effects on fatty acid and cholesterol metabolism can be uncoupled.

As we expected based on previously published work [9,10] and the observation that plasma cholesterol levels, blood leukocyte numbers and the extent of in vivo foam cell formation are not changed by SGC707 treatment, atherosclerotic lesion susceptibility was not modified by pharmacological inhibition of PRMT3 activity. Interestingly, PRMT3 has recently emerged as a putative novel target in the context of atherosclerosis and cardiovascular disease in humans. Chen et al. detected a 2-fold higher mRNA expression of PRMT3 in myocardial tissue from patients suffering from cardiovascular disease as compared to that

from subjects without atherosclerotic vessel disease [27]. In addition, human association studies by Shendre et al. have linked variation in the PRMT3 gene to a change in common carotid intima-media thickness (cCIMT), a measure of subclinical atherosclerosis [28]. Shendre et al. furthermore showed that the local European ancestry region in the PRMT3 gene is associated with a ~2 times higher stroke risk in African Americans [28]. This observational data suggest a role for PRMT3 in atherosclerosis. It is noteworthy that besides its proposed function as nuclear cofactor, PRMT3 belongs to the family of protein arginine *N*-methyltransferase enzymes that transfer methyl groups to the arginine residues of histones and other proteins to produce asymmetric dimethylarginine (ADMA) and, to a minor extent, symmetric dimethylarginine (SDMA). ADMA is a potent inhibitor of the formation of the anti-atherogenic agent nitric oxide [29]. Accordingly, ADMA increases atherosclerosis susceptibility in wild-type and apoE knockout mice [30,31]. In support of a negative impact of ADMA on atherosclerosis outcome in humans, high plasma ADMA levels serve as an independent predictor of high IMT levels in a variety of clinical settings [32,33]. Moreover, subjects in the highest quartile for plasma ADMA levels display a 3.9-fold increased risk for acute coronary events [34]. From our current study it can be concluded that complete inhibition of PRMT3 activity does not affect ADMA functionality in the cardiovascular context as we did not measure an effect on atherosclerosis outcome. It should however, be taken into account that we administered a dose of the PRMT3 inhibitor at which we aimed to be able to measure an effect on hepatic triglyceride accumulation. Although the hepatic steatosis extent was effectively lowered, it is currently unclear whether the dose of 10 mg kg^{-1} SGC707 is also sufficiently high to interfere with the ADMA/nitric oxide system. We did not detect an effect on systemic/plasma ADMA levels (data not shown). However, this does not necessarily exclude a potential (undetermined) impact of the chronic SGC707 treatment at an individual cellular level, i.e. in the aortic vessel wall. Further dedicated research, i.e. on vessel wall reactivity, may provide better insight in the potential of SGC707 to functionally modulate the body's ADMA/nitric oxide status and uncover the relevance in the cardiovascular disease setting, especially also since redundancy between the different PRMT family members has been suggested [35].

An interesting observation during our studies was that SGC707-treated mice, in marked contrast to control-treated mice, did not gain additional weight during the six week Western-type diet feeding period. Brown adipose tissue has emerged as a potential target to combat obesity due to its ability to burn fatty acids to produce heat, thereby eliminating storage of fat in white adipose tissue [36,37]. Since we did not primarily intend to investigate the effect of chronic SGC707 exposure on obesity development, a full metabolic profiling of the mice is unfortunately lacking. As such, we do not known the exact food intake nor the extent of heat produced by brown adipose tissue in the two groups of mice. Previous studies by Chen et al. have shown that exposure of C3H10T1/2 murine mesenchymal progenitor cells to the PRMT3 inhibitor compound 14u does not affect the ability of these cells to differentiate into brown adipocytes in vitro [38]. However, we observed a striking increase in browning of the subcutaneous white adipose tissue depot, which was paralleled by a marked increase in white adipose tissue UCP1 transcript levels. The decreased body weight gain can thus theoretically be the result of a higher heat production instead of fatty acid storage in white adipose tissue. However, dedicated in vivo studies are clearly warranted to decipher the exact function of PRMT3 in obesity development. The lower final body weight in SGC707-treated mice was also paralleled by a small change in the relative number of adipocytes in gonadal white adipose tissue. Strikingly, the change in gonadal white adipose tissue phenotype did not coincide with a decrease in the expression levels of the lipogenic genes SREBP-1c, FAS, ACC1, and SCD1, as we would have expected from our previous findings regarding PRMT3 functionality in liver [10]. The mRNA expression levels of LPL and CD36 were – however – lowered in gonadal white adipose tissue after SGC707 treatment. Adipose tissue-specific LPL deficiency does not change the obesogenic potential of mice [39]. In contrast, CD36 total body knockout mice as compared to their wild-type counterparts exhibit reduced adiposity in response to a high fat diet challenge, which appears to be driven by a reduction in the adipocyte uptake of lipoprotein-derived fatty acids and the associated reduction in white adipose tissue weight [40,41]. From these combined findings, it can be hypothesized that (1) the lipogenesis regulatory function of PRMT3 is perhaps restricted to hepatocytes and (2) that SGC707 treatment may actually decrease obesity development by lowering adipose tissue fatty acid uptake and switching white adipocytes to a more brown phenotype.

In conclusion, we have shown that treatment with the PRMT3 inhibitor SGC707 reduces hepatic steatosis without a negative impact on atherosclerosis susceptibility in hyperlipidemic mice. As such, our findings highlight that PRMT3 inhibition may constitute a novel therapeutic approach to limit the development of fatty liver disease in humans. Furthermore, the unanticipated decrease in body weight gain and changes in white adipose tissue associated with chronic SGC707 treatment imply a potential novel role for PRMT3 in white adipose tissue homeostasis and adipocyte function, which has to be validated in further research.

Supplementary data to this article can be found online at https://doi.org/10.1016/j.bbadis.2019.02.012.

Transparency document

The Transparency document associated with this article can be found, in online version.

Acknowledgements

We thank the other members of the Van Eck group for their practical support during the experiments. We acknowledge the support from the Netherlands CardioVascular Research Initiative: the Dutch Heart Foundation, Dutch Federation of University Medical Centers, the Netherlands Organization for Health Research and Development and the Royal Netherlands Academy of Arts and Sciences for the GENIUS project “Generating the best evidence-based pharmaceutical targets for atherosclerosis” [CVON2011-19]. This study was supported by the Netherlands Organization for Scientific Research [VICI Grant 91813603]. Miranda Van Eck is an Established Investigator of the Netherlands Heart Foundation [Grant 2007T056].

References

[1] K.L. Donnelly, C.I. Smith, S.J. Schwarzenberg, J. Jessurun, M.D. Boldt, E.J. Parks, Sources of fatty acids stored in liver and secreted via lipoproteins in patients with nonalcoholic fatty liver disease, J. Clin. Investig. 115 (5) (2005) 1343–1351.
[2] P. Angulo, Nonalcoholic fatty liver disease, N. Engl. J. Med. 346 (16) (2002) 1221–1231.
[3] F. Angelico, M. Del Ben, R. Conti, S. Francioso, K. Feole, D. Maccioni, et al., Non-alcoholic fatty liver syndrome: a hepatic consequence of common metabolic diseases, J. Gastroenterol. Hepatol. 18 (5) (2003) 588–594.
[4] C. Postic, J. Girard, Contribution of de nove fatty acid synthesis to hepatic steatosis and insulin resistance: lessons from genetically engineered mice, J. Clin. Investig. 118 (3) (2008) 829–838.
[5] J.R. Schultz, H. Tu, A. Luk, J.J. Repa, J.C. Medina, L. Li, et al., Role of LXRs in control of lipogenesis, Genes Dev. (2000) 2831–2838.
[6] J.J. Repa, G. Liang, J. Ou, Y. Bashmakov, J.A. Lobaccaro, I. Shimomura, et al., Regulation of mouse sterol regulatory by oxysterol receptors, LXRa and LXRb, Genes Dev. (2000) 2819–2830.
[7] A. Venkateswaran, B.A. Laffitte, S.B. Joseph, P.A. Mak, D.C. Wilpitz, P.A. Edwards, et al., Control of cellular cholesterol efflux by the nuclear oxysterol receptor LXRa, Proc. Natl. Acad. Sci. U. S. A. 97 (22) (2000) 12097–12102.
[8] R.K. Tangirala, E.D. Bischoff, S.B. Joseph, B.L. Wagner, R. Walczak, B.A. Laffitte, et al., Identification of macrophage liver X receptors as inhibitors of atherosclerosis, Proc. Natl. Acad. Sci. U. S. A. 99 (18) (2002) 11896–11901.
[9] D. Kim, M. Park, S. Lim, J. Park, K. Yoon, H. Han, et al., PRMT3 regulates hepatic lipogenesis through direct interaction with LXRa, Diabetes 64 (2015) 60–71.
[10] J.E. Nahon, C. Groeneveldt, J.J. Geerling, M. Van Eck, M. Hoekstra, Inhibition of PRMT3 activity selectively impairs LXR-driven transcription of hepatic lipogenic genes in vivo, Br. J. Pharmacol. 175 (15) (2018) 3175–3183.

[11] A. Grefhorst, B.M. Elzinga, P.J. Voshol, T. Plo, T. Kok, V.W. Bloks, et al., Stimulation of lipogenesis by pharmacological activation of the liver X receptor leads to production of large, triglyceride-rich very low density lipoprotein particles, J. Biol. Chem. 277 (37) (2002) 34182–34190.
[12] J. Folch, M. Lees, G.H. Sloane Stanley, A simple method for the isolation and purification of total lipides from animal tissues, J. Biol. Chem. 226 (1) (1953) 497–509.
[13] R. Out, M. Hoekstra, R.B. Hildebrand, J.K. Kruit, I. Meurs, Z. Li, et al., Macrophage ABCG1 deletion disrupts lipid homeostasis in alveolar macrophages and moderately influences atherosclerotic lesion development in LDL receptor-deficient mice, Arterioscler. Thromb. Vasc. Biol. 26 (10) (2006) 2295–2300.
[14] R. Out, W. Jessup, W. Le Goff, M. Hoekstra, I.C. Gelissen, Y. Zhao, et al., Coexistence of foam cells and hypocholesterolemia in mice lacking the ABC transporters A1 and G1, Circ. Res. 102 (1) (2008) 113–120.
[15] M. Hoekstra, J.K. Kruijt, M. Van Eck, T.J.C. van Berkel, Specific gene expression of ATP-binding cassette transporters and nuclear hormone receptors in rat liver parenchymal, endothelial, and Kupffer cells, J. Biol. Chem. 278 (28) (2003) 25448–25453.
[16] P. Chomczynski, N. Sacchi, Single-step method of RNA isolation by acid guanidinium extraction, Anal. Biochem. 162 (1987) 156–159.
[17] M.N. Bradley, C. Hong, M. Chen, S.B. Joseph, D.C. Wilpitz, X. Wang, et al., Ligand activation of LXR beta reverses atherosclerosis and cellular cholesterol overload in mice lacking LXR alpha and apoE, J. Clin. Investig. 117 (8) (2007) 2337–2346.
[18] H.Ü. Kaniskan, M.M. Szewczyk, Z. Yu, M.S. Eram, X. Yang, K. Schmidt, et al., A potent, selective and cell-active allosteric inhibitor of protein arginine methyltransferase 3 (PRMT3), Angew. Chem. Int. Ed. Eng. 54 (17) (2015) 5166–5170.
[19] Y. Takahashi, T. Fukusato, Histopathology of nonalcoholic fatty liver disease/nonalcoholic steatohepatitis, World J. Gastroenterol. 20 (42) (2014) 15539–15548.
[20] E.A. Craig, Z. Yan, Q.J. Zhao, The relationship between chemical-induced kidney weight increases and kidney histopathology in rats, J. Appl. Toxicol. 35 (7) (2015) 729–736.
[21] K. Bonham, S. Hemmers, Y.H. Lim, D.M. Hill, M.G. Finn, K.A. Mowen, Effects of a novel arginine methyltransferase inhibitor on T-helper cell cytokine production, FEBS J. 277 (9) (2010) 2096–2108.
[22] K.A. Mowen, B.T. Schurter, J.W. Fathman, M. David, L.H. Glimcher, Arginine methylation of Nip45 modulates cytokine gene expression in effector T lymphocytes, Mol. Cell 15 (4) (2004) 559–571.
[23] E. Ammirati, D. Cianflone, V. Vecchio, M. Banfi, A.C. Vermi, M. De Metrio, et al., Effector memory T cells are associated with atherosclerosis in humans and animal models, J. Am. Heart Assoc. 1 (1) (2012) 27–41.
[24] Z. Mallat, S. Taleb, H. Ait-Oufella, A. Tedgui, The role of adaptive T cell immunity in atherosclerosis, J. Lipid Res. 50 (2009) S364–S369.
[25] L.K. Juvet, S.M. Andresen, G.U. Schuster, K.T. Dalen, K.A.R. Tobin, K. Hollung, et al., On the role of liver X receptors in lipid accumulation in adipocytes, Mol. Endocrinol. 17 (2) (2003) 172–182.
[26] T.M. Stulnig, K.R. Steffensen, H. Gao, M. Reimers, K. Dahlman-Wright, G.U. Schuster, et al., Novel roles of liver X receptors exposed by gene expression profiling in liver and adipose tissue, Mol. Pharmacol. 62 (6) (2002) 1299–1305.
[27] X. Chen, F. Niroomand, Z. Liu, A. Zankl, H.A. Katus, L. Jahn, et al., Expression of nitric oxide related enzymes in coronary heart disease, Basic Res. Cardiol. 101 (4) (2006) 346–353.
[28] A. Shendre, H. Wiener, M.R. Irvin, D. Zhi, N.A. Limdi, E.T. Overton, et al., Admixture mapping of subclinical atherosclerosis and subsequent clinical events among African Americans in two large cohort studies, Circ. Cardiovasc. Genet. 10 (2) (2017) e001569 (pii).
[29] P. Vallance, A. Leone, A. Calver, J. Collier, S. Moncada, Accumulation of an endogenous inhibitor of nitric oxide synthesis in chronic renal failure, Lancet 339 (8793) (1992) 572–575.
[30] H.B. Xiao, Z.C. Yang, S.J. Jia, N.S. Li, D.J. Jiang, X.H. Zhang, et al., Effect of asymmetric dimethylarginine on atherogenesis and erythrocyte deformability in apolipoprotein E deficient mice, Life Sci. 81 (1) (2007) 1–7.
[31] J. Jacobi, R. Maas, A.J. Cardounel, M. Arend, A.J. Pope, N. Cordasic, et al., Dimethylarginine dimethylaminohydrolase overexpression ameliorates atherosclerosis in apolipoprotein E-deficient mice by lowering asymmetric dimethylarginine, Am. J. Pathol. 176 (5) (2010) 2559–2570.
[32] M.H. Urban, P. Eickhoff, G.C. Funk, O.C. Burghuber, M. Wolzt, A. Valipour, Increased brachial intima-media thickness is associated with circulating levels of asymmetric dimethylarginine in patients with COPD, Int. J. COPD 12 (2017) 169–176.
[33] W. Xia, L. Xu, W. Xu, X. Wang, Y. Yao, Asymmetric dimethylarginine is associated with carotid atherosclerosis in patients with essential hypertension, Clin. Exp. Hypertens. 37 (5) (2015) 393–397.
[34] I.E.M. Bultink, T. Teerlink, J.A. Heijst, B.A.C. Dijkmans, A.E. Voskuyl, Raised plasma levels of asymmetric dimethylarginine are associated with cardiovascular events, disease activity, and organ damage in patients with systemic lupus erythematosus, Ann. Rheum. Dis. 64 (9) (2005) 1362–1365.
[35] S. Dhar, V. Vemulapalli, A.N. Patananan, G.L. Huang, A. Di Lorenzo, S. Richard, et al., Loss of the major type i arginine methyltransferase PRMT1 causes substrate scavenging by other PRMTs, Sci. Rep. 3 (2013) 1–6.
[36] M.P.B. Moonen, E.B.M. Nascimento, W.D. van Marken Lichtenbelt, Human brown adipose tissue: underestimated target in metabolic disease? Biochim. Biophys. Acta Mol. Cell Biol. Lipids 1864 (1) (2019) 104–112.
[37] J.R. Ruiz, B. Martinez-Tellez, G. Sanchez-Delgado, F.J. Osuna-Prieto, P.C.N. Rensen, M.R. Boon, Role of human Brown fat in obesity, metabolism and cardiovascular disease: strategies to turn up the heat, Prog. Cardiovasc. Dis. 61 (2) (2018) 232–245.
[38] Y. Chen, J. Kim, R. Zhang, X. Yang, Y. Zhang, J. Fang, et al., Histone demethylase LSD1 promotes adipocyte differentiation through repressing Wnt signaling, Cell Chem. Biol. 23 (10) (2016) 1228–1240.
[39] I. Garcia-Arcos, Y. Hiyama, K. Drosatos, K.G. Bharadwaj, Y. Hu, N.H. Son, et al., Adipose-specific lipoprotein lipase deficiency more profoundly affects brown than white fat biology, J. Biol. Chem. 288 (20) (2013) 14046–14058.
[40] L. Cai, Z. Wang, A. Ji, J.M. Meyer, D.R. van der Westhuyzen, Scavenger receptor CD36 expression contributes to adipose tissue inflammation and cell death in diet-induced obesity, PLoS One 7 (5) (2012) e36785.
[41] I.O. Vroegrijk, J.B. van Klinken, J.A. van Diepen, S.A. van den Berg, M. Febbraio, L.K. Steinbusch, et al., CD36 is important for adipocyte recruitment and affects lipolysis, Obesity (Silver Spring) 21 (10) (2013) 2037–2045.